A Thesis

On

Study on room temperature ferromagnetism behavior of Cr doped CdSe diluted magnetic nanostructures

Submitted in the partial fulfillment of requirement for the award of the

Degree of

Master of Science (Physics)

Submitted by

Amit Bansal

Roll No.: 300904002

Supervisor

Dr. N.K.Verma

Senior Professor of Physics

Under

School of Physics and Materials Science

Thapar University, Patiala–147004

JULY 2011

Certificate

This is to certify that the thesis entitled, **"Study on room temperature ferromagnetism behavior of Cr doped CdSe diluted magnetic nanostructures"** submitted by **Mr. Amit Bansal (300904002)** of **M.Sc (Physics),** Thapar University, Patiala was carried out byhim under my supervision. He has not submitted this material for credit towards any other degree at Thapar University,Patiala or any other University.

(Dr. N.K. Verma)

Senior Professor

School of Physics and Materials Science

Thapar University, Patiala-147 004

Countersinged by

(Dr.O.P. Pandey)

Professor and Head

School of Physics and Materials Science

Thapar University, Patiala

(Dr. S. K. Mohapatra)

Dean of Academic Affairs

Thapar University, Patiala

Acknowledgement

Aparts from the efforts of me, the success of my project depends largely on the encouragement and guidelines of many others. On submission of my thesis, I would like to express my esteemed sense of gratitude and respect to my guide **Dr. N K Verma, Senior Professor, School of Physics and Material Science, Thapar University, Patiala,** for his keen interest and valuable guidance, strong motivation and constant encouragement during the course of the work. I thank him from the bottom of my heart for introducing me to fundamentals of Nanoscience. I am sure that the knowledge gained through my association under his supervision shall help me to realize my goals in life.

I am greatful to **Mr. Gurmeet Singh Lotey** for their kind help & suggestions at various stages of my thesis work.

I am also greatful to **Mr. Sanjeev Kumar,Mr. Jaspal Singh, Ms. Lavanaya Khanna and Ms. Manveen Kaur** for their kind help & suggestions at various stages of my thesis work.

I am thankful to **Mr. Rohit Singh** of School of Chemistry and Biochemistry and **my friends** for their kind help, inspiration and encouragement at every stage during the project report work.

Finally, I would like to express my deepest gratitude to **my parents,** without whom I am nothing, to provide me great opportunities, everlasting support, encouragement and a lot of love.

Amit Bansal

Abstract

Diluted magnetic semiconductors (DMS), are semiconductors in which a magnetic impurity is intentionally introduced; a small fraction of the native atoms in the hosting non-magnetic semiconductor material is replaced by magnetic atoms.

Incorporating of magnetic ions in semiconductors nanocrystallites, host materials modifying the optical, magnetic, and electronic properties. DMSs are ideal material for spin based electronics, i.e., Spintronics. The realization of functional spintronic devices requires materials with ferromagnetic ordering at operational temperatures compatible with existing semiconductor materials. Being a ferromagnetic semiconductor with favorable experimental properties, dilute magnetic semiconductors will promisingly suit this need.

Pure and Cr-doped CdSe dilute magnetic semiconductors have been synthesized by solvothermal route. The particles were capped with 2-marcaptoethanol to achieve the stability. These samples are characterized by X-ray diffraction for structural and phase analysis. The optical properties were studied by photoluminescence; UV-visible absorption spectroscopy and Fourier transform infrared spectroscopy. The morphology of the synthesized nanoparticles was analyzed by Scanning electron microscope and transmission electron microscope. The magnetic measurements were done by vibrational sample magnetometer. The pure CdSe nanoparticles show diamagnetic behavior but Cr doped CdSe nanoparticle shows ferromagnetic behavior.

Contents **Page Number**

Certificate……ii

Acknowledgement……...iii

Abstract……....iv

List of figures and tables……vii

Chapter 1: Introduction…….....1

Chapter 2: Literature Review…….....5

Chapter 3: Objectives……..9

3.1 Gaps in study……....9

3.2 Objectives……9

3.3 Methodology……9

Chapter 4: Experimental and Instrumentation…….....11

4.1 Synthesis of nanomaterials……...11

4.1.1 Bottom up approach……11

4.1.2 Top down approach…….....11

4.1.3 Synthesis of CdSe nanostructures……...12

4.2 Characterization Techniques……...13

4.2.1 X-Ray Diffraction (XRD)……...13

4.2.2 Scanning Electron Microscopy (SEM) & Energy Dispersive X-ray Spectroscopy (EDAX)…….....14

4.2.3 Transmission Electron Microscope (TEM)…….....17

4.2.4 UV-Visible absorption spectroscopy……..…….....18

4.2.5 Photoluminescence (PL)……..…….....19

4.2.6 Fourier Transform Infrared Spectroscopy…….…….....……20

4.2.7 Vibrational Sample Magnetometer (VSM)…….....22

Chapter 5 Results and Discussion…….24

5.1 Structural and phase analysis.....24

5.2 Morphological Study.....25

5.2.1 SEM and EDAX analysis.....25

5.2.2 TEM analysis…….27

5.3 UV-Visible absorption study……...27

5.4 Photoluminescence study……....28

5.5 FTIR study…….....29

5.6 Magnetic study……..…….…….....30

5.7 Conclusions…….30

References…….……c

List of Figures Page Number

Figure 1.1 Semiconductor host doped with magnetic ions 3

Figure 1.2 (a) Wurtzite (hexagonal) and (b) zinc blende (cubic) crystal structure of CdSe 4

Figure 4.1 Bragg's law of diffraction 14

Figure 4.2 Schematic of different components of SEM 15

Figure 4.3 Different processes takes place when an electron interact with atom 17

Figure 4.4 Schematic of different components of TEM 18

Figure 4.5 Schematic of UV-Visible spectrometer 19

Figure 4.6 Interaction of light with semiconductor 20

Figure 4.7 Schematic of FTIR 21

Figure 4.8 Schematic of components of VSM 23

Figure 5.1 XRD pattern of CdSe and Cr doped CdSe nanoparticles 24

Figure 5.2 Variation of crystallites size with doping 25

Figure 5.3 SEM micrograph (a) pure CdSe and Cr doped CdSe (b) 1% (c) 3% (d) 5% nanoparticles 26

Figure 5.4 EDAX spectra of (a) pure CdSe (b) 1% and (c) 3% Cr doped CdSe nanoparticles 26

Figure 5.5 (a) TEM micrograph of pure CdSe nanoparticles 27

(b) Size distribution of CdSe nanoparticles

Figure 5.6 UV-Visible absorption spectra for pure and Cr doped CdSe nanoparticles 27

Figure 5.7 PL spectra of pure and Cr doped CdSe nanoparticles 28

Figure 5.8 FTIR spectra of pure CdSe and Cr doped CdSe nanoparticles 29
capped with 2-marcaptoethanol

Figure 5.9 Magnetic hysteresis (M–H) loops for pure CdSe and 5% Cr doped 30
CdSe nanoparticles measured at 300 K

Chapter 1 Introduction

Nanotechnology is the manipulation of materials or devices atom by atom through control of structure at nanoscale. It deals with materials having at least one dimension between 1 to 100 nm and involves developing materials or devices within that size [1]. Nanomaterials exhibit different physical, chemical and biological properties from their bulk counterpart and having great applications in various fields. The nanomaterials have attracted a great attention due to their size dependent physical, chemical, magnetic, electronic, optical and biological properties which arises due to large surface to volume ratio and quantum confinement effects.

The materials joining both the characteristics of semiconductors and magnetic materials, known as Dilute Magnetic Semiconductors (DMSs) or semimagnetic semiconductors. In recent years, DMSs have emerged as a much researched field due to the possibility of manipulating charge and spin degree of freedom. The DMSs materials are believed to be the ideal candidate for spintronic applications [2, 3]. Spintronics is spin based electronics, which is the promising field in research area and has impact on future technology. For most of the twentieth century, it was known that electrons which mediate electrical current in electronic circuitry possess angular momentum but, yet no practical use has been made of this. With the dawn of the new millennium, has emerged a novel technology which exploits electron spin and uses it to differentiate electrical carriers into two different types according to whether their spin projection onto a given quantization axis is ±1/2. Spin-electronic devices function by transferring magnetic information from one part of the device to another by using nanoscale magnetic elements (mesomagnets) to encode it onto (and subsequently read it off) the itinerant electron spin channels. This coding may be changed by remagnetizing the mesomagnets thus enabling the creation of electronic components whose characteristics may be engineered to respond to applied magnetic fields.

The major challenges for semiconductor based spintronic devices is to develop suitable novel spin-polarized magnetic semiconducting materials that will effectively allow spin-polarized carriers to be injected, transported, and manipulated [4]. Therefore searching for new materials has become crucial from the viewpoints of both fundamental research and practical applications. The researchers are trying to exploit the 'spin' of the electrons along with its electronic charge to create a remarkable new generation of 'Spintronic' devices which

will be smaller, more versatile in nature and more robust than those currently used [5]. There are two major criteria for selecting the most promising materials for semiconductor spintronics. Firstly, the ferromagnetism should be retained to practical temperatures (i.e. $\geq$ 300 K). Secondly, it would be a major advantage if there were already an existing technology base for the material in other applications. The significance achievement in the area of spintronics is Giant Magneto Resistance (GMR) effect discovered by Abert Fert and Peter Grunberg [6, 7]. The change in electrical resistance of some materials in response to an applied magnetic field is known as magneto resistance but when magnetic field is applied to thin films composed of alternate ferromagnetic and non-ferromagnetic layers such as Fe/Cr, a large change in resistance has been observed known as GMR. This effect revolutionized the minds of the researchers to quest for suitable materials for read and write head memory devices [8].

Study of DMSs have centered mostly on II-VI semiconductors, such as CdSe, CdTe and ZnSe in which the valence of the cations matches that of the common magnetic ions such as Mn. Although this phenomenon makes these DMSs relatively easy to prepare in bulk form as well as in thin epitaxial layers, II-VI based DMSs have been difficult to dope to create p- and n-type, which made the material less attractive for applications. Moreover, the magnetic interaction in II-VI DMSs is dominated by the antiferromagnetic exchange among the Mn spins, which results in the paramagnetic, antiferromagnetic, or spin-glass behavior of the material. It was not possible until very recently to make II-VI DMS ferromagnetic at low temperature.

Dilute magnetic semiconductors (DMS) are semiconductors where a fraction of the cations in the lattice are replaced substitutionally by magnetic ions (figure 1.1). The atomic spin on these magnetic dopants is interacted with the carriers in the lattice to bring about global ferromagnetic order in the material. They have unusual magnetic characteristics due to the presence of isolated magnetic ions in semiconducting lattice. DMS were interesting from both a theoretical, as well as a technological point of view. Unlike metals, semiconductors allow properties such as band gap and carrier concentration to be tailored to fit the application. Further, if the magnetism in the material is related to the carrier concentration, then it might be possible to electrically tune the magnetism. This could lead to a new functionality of gate-controlled ferromagnetism. Although physics of the magnetism was thoroughly investigated in II-VI DMS, they were not suitable for technological applications.

One of the reasons for this was that ferromagnetic order could not be achieved at high temperatures in these materials.

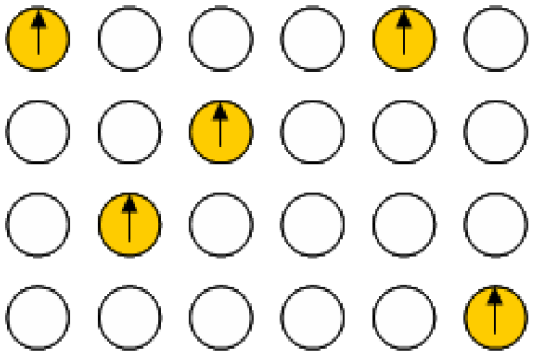

Figure 1.1 Semiconductor host doped with magnetic ions.

CdSe is one of the most important II-VI semiconductor material with direct band gap Eg = 1.74eV at 300K, electron mobility of 450-900 cm^2/Vs and melting point is 1239^0C. Semiconductor nanocrystals such as CdSe are called quantum dots (QD) when the size of the first Bohr radius exceeds the crystallite size (D), leading to quantum confinement effects such as increase in the band-gap (Eg) with decrease in crystallite size (D). For the CdSe nanoparticles, Eg can be tuned to cover the whole visible range by change in D, thus making this system potentially useful for solar cells, photodetectors, optoelectronics, light emitting diodes, lasers and photoelectrochemical cells. More recently, induced magnetism has been reported for CdSe nanoparticles and attributed to a variety of sources, including the existence of dangling bonds, induction by surface ligands, and even defects in the CdSe particles. Adding more complexity to these observations is the fact that none of these studies systemically investigated both size and surface ligand effects, and few reports claim that the observed magnetism is due to ferromagnetic ordering [9]. The magnetic behavior of the CdSe nanoparticles can be enhanced by variation of the functional group of the passivating surfactant.

The synthesis of DMSs nanostructures are of great interest as semiconducting and magnetic properties are combined in one and the same nanostructure, therefore ordered arrays of nanometer-sized magnetic semiconductors are promising components for magneto or spin electronics (e.g., magnetic hard disk media, non-volatile computer memory chips) devices. The miniaturization of these DMSs compounds lead to zero, one, or two-dimensional nanostructures such as quantum dots, quantum wires, and quantum wells. It has been found that the electronic as well as the magnetic properties of such DMSs nanostructures are

affected by the reduced dimensionality. The understanding of change in the magnetic behaviour at reduced dimensions is essential for device miniaturization.

However to a date, a little, if any, efforts has been expended in research associated with room temperature ferromagnetism study on transition metal doped CdSe nanoparticles. Also, the studies on the effect of size on magnetic properties of transition metal doped CdSe nanoparticles have not been reported.

CdSe has two types of crystal structures i.e Wurtzite (hexagonal) crystal structure and zinc blende (cubic) crystal structure as shown in figure 1.2

(a) **(b)**

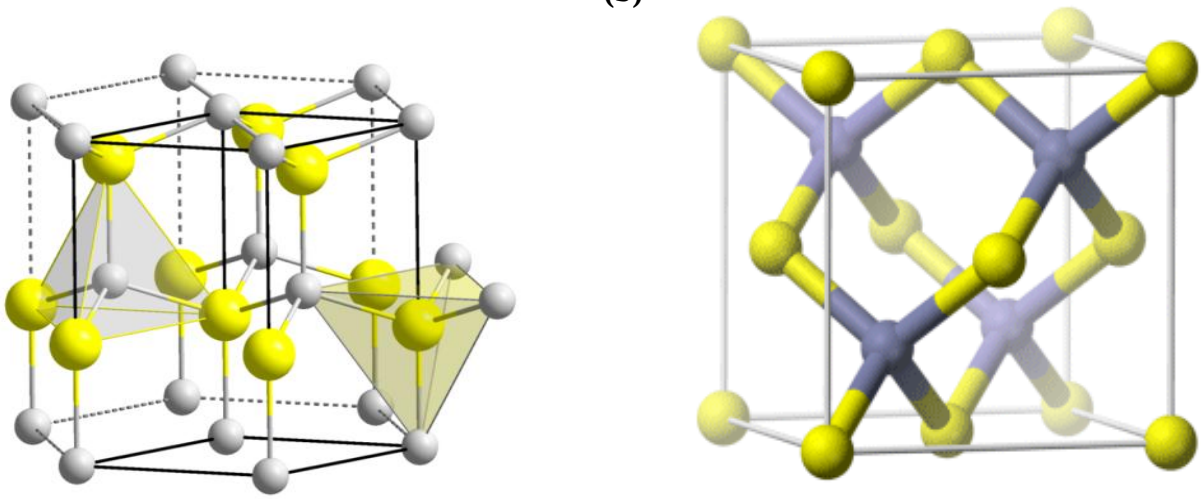

Figure 1.2 (a) Wurtzite (hexagonal) and (b) zinc blende (cubic) crystal structure of CdSe.

The literature was reviewed in detail, in order to learn the optimum information as to the genesis and the technical applications of the work and is given as under:

The dilute magnetic semiconductors (DMSs) are the promising candidates for the "Spintronics" device applications. The first report on ferromagnetic and semiconducting properties of $CrBr_3$ was reported in 1960 but the Curie temperature was found to be very low about 37 K. After this, studies on various materials like EuO, MnAs, MnSb, $CdCr_2S_4$, Sr_2FeMnO_6, Fe_3O_4, $YTiO_3$, $SeCuO_3$, $BiMnO_3$, have been reported, but a little improvement in Curie temperature was found [10].

Dietl et al. [11] in 2000 theoretically proposed number of materials that can show DMSs behaviour. But, the p-type GaN and ZnO semiconductor doped with 5% Mn shows room temperature ferromagnetism. After this prediction, a number of reports were published on room temperature ferromagnetic behaviour of different materials; III-V compounds, II-VI compounds, IV-VI compounds and VI compounds [12-14].

It is found that the II-VI and III-V doped semiconductors are found to be promising candidates for spintronic applications. But the major hindrance for the practical implementation of the spin concepts is the difficulty in preparing suitable materials with desired properties, which can serve as a high efficiency source of charge carriers with well defined spin, yet be compatible with existing semiconductor technologies. The much of the work has been done on II-VI semiconductor nanoparticles doped with magnetic impurities are the most promising DMS materials. Among these, the extensive research has been focussed on CdSe nanoparticles as a host material, and doping of suitable ions such as transition metal or rare earth metals to explore its DMS behaviour [15]. The CdSe nanoparticles being a direct band gap semiconductor shows very interesting properties such as energy band gap tuning, optical, electronic, and electrical properties just by varying its dimensions and addition of suitable dopant.

Mikulec et al. [16] in 2000 described, the problem related doping of transition metals in II-VI compound semiconductors nanocrystals. The spectroscopic analysis of Mn doped CdSe nanocrystals has been done. The Electron Paramagnetic Resonance (EPR) study revealed that the most of the dopant atoms reside on the surface layers of the inorganic lattice. The optical study gives that the Mn doped CdSe quantum dot behaves like undoped

quantum dot in the presence of external magnetic field because of the interaction of electron/hole spin with paramagnetic impurities.

Hanif et al. [17] in 2002 reported the magnetic ordering in Co-doped CdSe DMSs quantum dots. The structural and magnetic properties of Co-doped CdSe quantum dots were elaborated. The super paramagnetic behavior of quantum dots (QDs) were observed due the anti-ferromagnetic (AFM) interactions which can be arise between Co spins in an isolated particle (intra-particle) or AFM interactions between spins in neighboring particles (inter-particle).The enhanced values of exchange integral by an order of magnitude in the QDs compared to the bulk, may be due to the result from an increase in Co d-orbital overlap with the CdSe valence band minimum. The correlation of studies suggest that the observed enhancement in magnetic super-exchange interactions between Co^{2+} dopant ions in CdSe quantum dots are due to changes in the nature of coupling in size-restricted materials.

Jian et al. [18] in 2003 studied that dynamic magnetic properties of $Cd_{1-x}Mn_xSe$ dilute magnetic semiconductor. The Electron Paramagnetic Resonance (EPR) spectra revealed that the interactions between the Mn-Mn dopants are enhanced and spin coherence length is improved due to quantum confinement effect in quantum dots.

Meulenberg et al. [19] in 2004 reported the electronic and chemical structure of Cu doped CdSe nanocrystals by employing X-ray absorption near edge spectroscopy (XANES). This study revealed that in the local environment of Cu, in CdSe it exist in +1 oxidation state, which leads to charge imbalance. As a result of this the Se density of state changes due to Se d-hybridization with Cu gives rise to interesting optical properties. The charge imbalance present in Cu doped CdSe nanocrystals induces defects, and the PL spectra get quenched as the doping concentration is increased.

Magana et al. [20] in 2006 reported the super paramagnetic behaviour of Mn doped CdSe quantum dots. The as grown Mn^{2+} doped of CdSe quantum dots from a cubic single source precursor that is super paramagnetic in nature with a blocking temperature of 40 K, following thermal annealing. But before thermal annealing, the 4 nm Mn doped CdSe (1% Mn) quantum dots show paramagnetic behaviour between 300 and 2 K, with a weak antiferromagnetic exchange. With the thermal annealing, the quantum dots show high-temperature ferromagnetic exchange. The switching-on of super paramagnetic behaviour is due to the migration and formation of $(Se\text{-}Mn\text{-}Se\text{-}Mn\text{-}Se\text{-}Mn)_n$ centres within the nanocrystals that exhibit coupled magnetic moments.

Archer et al. [21] in 2007 reported the sp-d exchange interactions which are responsible for magnetism in Mn^{2+} and Co^{2+} doped CdSe quantum dots. The doping and

existence of giant excitonic Zeeman effect splitting in both Mn^{2+} and Co^{2+} doped CdSe quantum dots were demonstrated by magnetic circular dichroism spectroscopy (MCD). The study confirmed that such transition metal doped CdSe nanocrystals are the promising candidates for studying the spin based effects and are relevant to spin based information storage processing.

Singh et al. [22] in 2008 presented the room temperature ferromagnetism in thiol-capped CdSe nanoparticles. Also, the effect of Cu doping CdSe nanoparticles on magnetic properties has been explored. The well-defined hysteresis loop with saturation magnetization has been observed for pure thiol capped CdSe nanoparticles at room temperature. But with the addition of Cu ions in CdSe, the saturation magnetization increases at low concentration, then decreases consistently with increases in dopant concentration. At higher concentration of dopant ≈17.2% the magnetization decreases due to interaction between Cu-Cu ions which leads to antiferromagnetic character. Also, the observed magnetisation does not vary with temperature range 300-420K.

Beaulac et al. [15] reported the spin base electronics and photonics properties of Mn^{2+} doped CdSe quantum dots. The paper describes the progress in Mn^{2+} doped CdSe quantum dots; in development of free standing colloidal, basic electronic properties, self-assembly on nanocrystals, photoluminescence properties and giant Zeeman splitting. The effect of size in various physical, chemical, and magnetic properties was presented. It has been found that photon polarization in Mn^{2+} doped CdSe quantum dots can be converted to electron spin polarization and polarized spins recombine to yield circularly polarized photons.

Seehra et al. [23] observed size dependent ferromagnetism in trioctylphosphineoxide (TOPO) capped CdSe quantum dots. The ferromagnetic behaviour of these quantum dots is due to charge transfer from Cd ion d-band to the oxygen atoms of TOPO [24].

Singh et al. [25] presented the optical and magnetic properties of Fe substituted CdSe nanoparticles. The Mossbauer and EPR confirmed that Fe presented in +3 oxidation state in CdSe. The CdSe nanoparticles capped with thiol showed room temperature ferromagnetic behaviour. The saturation magnetisation in Fe doped CdSe nanoparticles increases upto 8.58 % dopant concentration. With further increase in Fe concentration ferromagnetic to paramagnetic behaviour transition observed. Also, with change in temperature the magnetization first increases upto 100 K and then decreases upto 200 K, after this saturation magnetization become constant. The magnetic behaviour of Fe doped CdSe nanoparticles have been explained on the basis of F-centre exchange mechanism i.e. bound magnetic polarons, charge imbalance, defects.

Sunil et al. [26] 2010 observed room temperature ferromagnetism in Ni doped CdSe nanoparticles synthesized by a wet chemical precipitation method. The magnetic studies revealed that pure CdSe nanoparticles (NPs) exhibit diamagnetic behaviour at 300 K, whereas 5% Ni doped CdSe NPs shows the mixed behaviour possess both the paramagnetic and ferromagnetic character.

Meulenberg et al. [27] reported the surface manipulation of the magnetic properties of CdSe quantum dots. The comparison of three surfactants such as hexadecylamine (HAD), trioctylphosphine-oxide (TOPO), and dodecanenitrile (DDN) were studied using XANES, Superconducting quantum interference device magnetometry (SQUID), and X-ray magnetic circular dichroism (XMCD) techniques. They give the evidence that a ∏-back bonding mechanism between the surface Cd atoms and the organic surfactants were responsible for observed magnetism in capped CdSe quantum dots.

Jun et al. [28] The DMSs are the very promising materials for future device applications which find technological importance and help to understand basic fundamentals. The transition metal doped CdSe semiconductor nanoparticles are found to be a one of promising candidate for spintronic applications. But from the application point of view, the low Curie temperatures (T_C) of the investigated DMSs represent a serious problem, and many efforts have been devoted to find ferromagnetic DMSs with T_C higher than room temperature.

But however little reports are available on room temperature magnetic study of CdSe nanoparticles.

Chapter 3 Objectives

3.1 GAPS IN STUDY

It has been found by reviewing literature that the following area is not well explored till now.

- Room temperature magnetic study of Cr doped CdSe nanoparticles.

3.2 OBJECTIVES

- ✓ Synthesis of Cr doped CdSe nanoparticles by solvothermal synthesis route.
- ✓ The characterization of synthesized CdSe nanoparticles; structurally by X-ray diffraction (XRD), morphologically by Scanning Electron Microscopy (SEM) and Transmission Electron Microscopy (TEM).
- ✓ Optical studies by UV-Visible spectroscopy, Photoluminescence (PL) and Fourier Transmission Infrared Spectroscopy (FTIR).
- ✓ Magnetic study by Vibrational Sample Magnetometer (VSM).

3.3 METHODOLOGY

Following steps will be taken to achieve the objectives:

- **Synthesis of Cr doped CdSe nanoparticles:** The synthesis of transition metal-doped CdSe will be done by solvothermal route. In this, the equimolar solution of cadmium chloride ($CdCl_2$) and Selenium (Se) powder is dissolved in ethylenediamine (en). Macaptoethanol is used as a capping agent. The mixture is transferred to an autoclave and the autoclave is placed in heating oven for 18h at 150^0C temperature. The dark reddish brown precipitates were obtained. As obtained precipitates were washed with ethanol and distilled water for several times. Finally dried the precipitates at 60^0C in hot air oven.

- **Structural Analysis:** XRD characterization will be done to know about the crystal structure, crystallinity, and crystallite size of synthesized powder.
- **Morphological Characterization**: The morphology of as synthesized samples will be examined by SEM and TEM.

- **Optical analysis:** UV-Visible spectroscopy will be carried out to know absorption, band gap, etc., photoluminescence (PL) analysis will be carried out to study optical transitions, defects in synthesized nanoparticles and FTIR will be done to study capping of surfactant in synthesized nanoparticles.

- **Magnetic measurements:** VSM measurements will be done to study the magnetic behavior of synthesized product.

Chapter 4 Experimental and Instrumentation

4.1 Synthesis of nanomaterials

The nano materials can be prepared by different method categorized viz. Bottom up and Top down.

4.1.1 Bottom up approach

A bottom-up approach refers to the build-up of a material from the bottom i.e. atom by atom, molecule by molecule, or cluster by cluster. In crystal growth such as atoms, ions and molecules, after impinging onto the growth surface, assemble into crystal structure one after another. Bottom up approach promises a better chance to obtain nanostructures with less defects, more homogeneous chemical composition and better short and long range ordering. Examples of bottom-up approach:

1. Solution combustion method
2. Sol-gel
3. Micro-emulsion
4. Reverse micelle
5. Chemical precipitation
6. Solvothermal/hydrothermal

4.1.2 Top down approach

A top-down approach is essentially the breaking down of a system into its compositional sub systems. In a top-down approach an overview of the system is first formulated, specifying but not detailing any first-level subsystems. Each subsystem is then refined in yet greater detail, sometimes in many additional subsystem levels, until the entire specification is reduced to base elements. Attrition or milling is a typical top-down method in making nanoparticle. Examples of top-down approach:

1. High energy milling
2. Chemical mechanical milling
3. Vapor phase condensation
4. Electro-explosion
5. Laser ablation
6. Sputtering

Bottom up approach is much better than Top down because bottom-up approach is driven mainly by the reduction of gibbs free energy, so that nanostructures and nanomaterials such produced are in a state closer to a thermodynamic equilibrium state. On the contrary, top-down approach most likely introduces internal stress, in addition to surface defects and contaminations.

4.1.3 Synthesis of CdSe nanostructures

Solvothermal technique: A solvothermal process can be defined as "a chemical reaction in a closed system in the presence of a solvent (aqueous and non-aqueous solution) at a temperature higher than that of the boiling point of such a solvent". Consequently a solvothermal process involves high pressures. The selected temperature depends on the required reactions for obtaining the target-material through the involved process.

Hydrothermal processes: Due in particular to the chemical composition of water as solvents are mainly appropriated to the preparation of hydroxides, oxihydroxides or oxides versus the temperature value. Solvothermal reactions are governed by different factors:

- ✓ The nature of the precursors, in particular their physico-chemical properties (solubility, thermal stability, etc)
- ✓ The nature of the solvent (chemical composition, physic-chemical properties, solvatation, polarity, viscosity, ability to stabilize some complexes as intermediate steps)
- ✓ The thermodynamical properties used during such a process (pressure and temperature)

Pressure and temperature can play an important role; some properties of solvent such as density, viscosity, etc. are changing drastically versus such parameters. Consequently the diffusion and reactivity of chemical species can be strongly affected. In a general way, solvothermal processes were developed in mild temperature conditions. The main chemical reaction-types involved in solvothermal processes are: hydrolysis, complex-formation, metathesis, and oxidation-reduction. The reaction-type governing the in-situ mechanisms is closely related to the optimization of the three main factors governing the process viz. chemical nature of precursors, physico-chemical properties of the solvent, thermodynamical conditions. Such an optimization depends on the final objective: synthesis of a novel material (thermodynamically stable or metastable), preparation of fine crystallites well defined in size, morphology and growth of single crystal.

The synthesis of transition metal (Cr)-doped CdSe will be done by solvothermal route. In this, the equimolar solution of cadmium chloride ($CdCl_2$) and Selenium (Se) powder is dissolved in ethylenediamine (en). Macaptoethanol is used as a capping agent. The mixture is transferred to an autoclave and the autoclave is placed in heating oven for 18h at 150^0C temperature. The dark reddish brown precipitates were obtained. As obtained precipitates were washed with ethanol and distilled water for several times. Finally dried the precipitates at 60^0C in hot air oven.

4.2 Characterization Techniques

The characterization of materials regarding determination of elemental composition, estimation of trace impurities, structural analysis, morphological analysis, dielectric analysis, magnetic analysis, identification of crystalline phases and information on crystal defects play an important role for the quality control and development of advanced materials. The nanostructures have been characterized by their structural, compositional, morphological, optical, magnetic and dielectric properties. The techniques include X-ray diffraction (XRD), Scanning Electron Microscopy (SEM) & Energy Dispersive X-rays Spectroscopy (EDAX), Transmission Electron Microscopy (TEM), UV-visible Absorption Spectroscopy, Photoluminescence (PL), Fourier Transformation Infrared Spectroscopy (FTIR) and Vibrational Sample Magnetometer (VSM).

4.2.1 X-Ray Diffraction

X-ray diffraction (XRD) is a versatile, non-destructive technique that reveals detailed information about the chemical composition and crystallographic structure of natural and synthesized materials. This technique is used to identify and characterize unknown crystalline materials. Monochromatic X-rays are used to determine the interplanar spacing of the unknown materials. Samples are analyzed as powders with grains in random orientations to insure that all crystallographic directions are "sampled" by the beam. When the Bragg conditions for constructive interference are obtained, a "reflection" is produced, and the relative peak height is generally proportional to the number of grains in a preferred orientation. When a crystal is bombarded with X-rays of a fixed wavelength and at certain incident angles, intense reflected X-rays are produced when the wavelengths of the scattered X-rays interfere constructively. In order for the waves to interfere constructively, the differences in the travel path must be equal to integral multiples of the wavelength. When this

constructive interference occurs, a diffracted beam of X-rays will leave the crystal at an angle equal to that of the incident beam. To illustrate this feature, consider a crystal with crystal lattice planar distances d. Where the travel path length difference between the ray paths of two beams (ABC and A'B'C') is an integer multiple of the wavelength, constructive interference will occur for a combination of that specific wavelength,

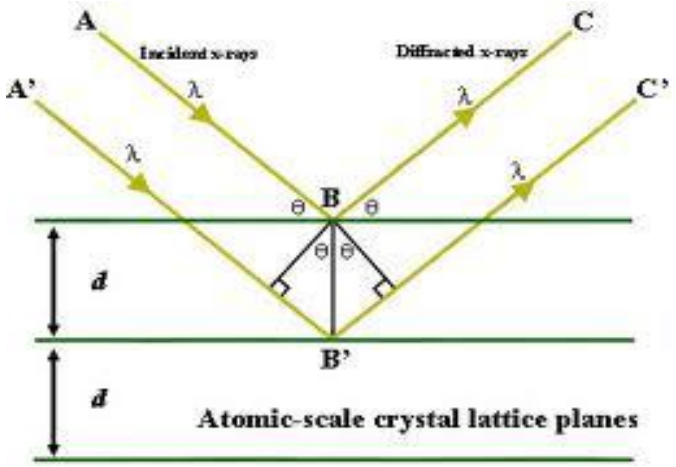

Figure 4.1 Bragg's law of diffraction

crystal lattice planar spacing and angle of incidence (θ). Each rational plane of atoms in a crystal will undergo refraction at a single, unique angle (for X-rays of a fixed wavelength). According to Bragg's Law i.e

$$2\,d\sin\theta = n\lambda$$

Where n is an integer that indicates the order of reflection, λ is the wavelength of the incident X- rays, d is the interplanar spacing of the crystal and θ is the angle of incidence.

Applications

- Degree of crystallinity
- Determination of the crystal structure
- Determination of crystallite size from peak broadening.

4.2.2 Scanning Electron Microscopy (SEM) & Energy Dispersive X-ray Spectroscopy (EDAX)

The scanning electron microscope (SEM) uses a focused beam of high-energy electrons to generate a variety of signals at the surface of solid specimens. The signals that derive from electron-sample interactions reveal information about the sample including external morphology, chemical composition, and crystalline structure and orientation of materials making up the sample. In most applications, data are collected over a selected area of the

surface of the sample, and a 2-dimensional image is generated that displays spatial variations in these properties. Areas ranging from approximately 1 cm to 5 microns in width can be imaged in a scanning mode using conventional SEM techniques (magnification ranging from 20X to approximately 30,000X, spatial resolution of 50 to 100 nm). The SEM is also capable of performing analyses of selected point locations on the sample; this approach is especially useful in qualitatively or semi-quantitatively determining chemical compositions (using EDS), crystalline structure, and crystal orientations (using EBSD).

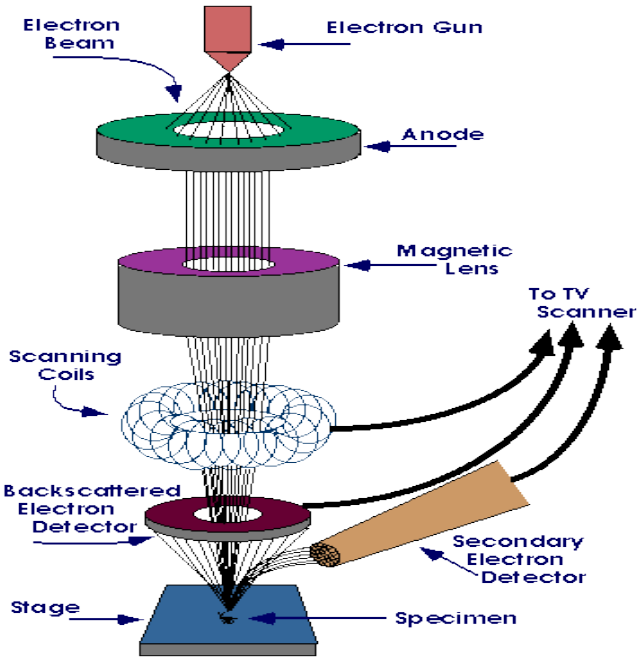

Figure 4.2 Schematic of different components of SEM

Accelerated electrons in an SEM carry significant amounts of kinetic energy, and this energy is dissipated as a variety of signals produced by electron-sample interactions when the incident electrons are decelerated in the solid sample. These signals include secondary electrons (that produce SEM images), backscattered electrons (BSE), diffracted backscattered electrons (EBSD that are used to determine crystal structures and orientations of minerals), photons (characteristic X-rays that are used for elemental analysis and continuum X-rays), visible light (cathodoluminescence CL), and heat. Secondary electrons and backscattered electrons are commonly used for imaging samples: secondary electrons are most valuable for showing morphology and topography on samples and backscattered electrons are most valuable for illustrating contrasts in composition in multiphase samples (i.e. for rapid phase discrimination). X-ray generation is produced by inelastic collisions of the incident electrons

with electrons in discrete ortitals of atoms in the sample. As the excited electrons return to lower energy states, they yield X-rays that are of a fixed wavelength (that is related to the difference in energy levels of electrons in different shells for a given element). Thus, characteristic X-rays are produced for each element in a mineral that is "excited" by the electron beam. SEM analysis is considered to be "non-destructive"; that is, x-rays generated by electron interactions do not lead to volume loss of the sample, so it is possible to analyze the same materials repeatedly.

EDAX systems are most commonly found on scanning electron microscopes (SEM-EDAX) and electron microprobes. This technique is used in conjunction with SEM and is not a surface science technique. An electron beam strikes the surface of a conducting sample. This causes X-rays to be emitted from the point the material. The energy of the X-rays emitted depends on the material under examination. The Energy dispersive X-ray spectroscopy (EDS, EDX or EDXRF) is an analytical technique used for the elemental analysis or chemical characterization of a sample. As a type of spectroscopy, it relies on the investigation of a sample through interactions between electromagnetic radiation and matter, analyzing X-rays emitted by the matter in response to being hit with charged particles. Its characterization capabilities are due in large part to the fundamental principle that each element has a unique atomic structure allowing X-rays that are characteristic of an element's atomic structure to be identified uniquely from each other. To stimulate the emission of characteristic X-rays from a specimen, a high energy beam of charged particles such as electrons or protons or a beam of X-rays, is focused into the sample being studied. At rest, an atom within the sample contains ground state (or unexcited) electrons in discrete energy levels or electron shells bound to the nucleus. The incident beam may excite an electron in an inner shell, ejecting it from the shell while creating an electron hole where the electron was. An electron from an outer, higher-energy shell then fills the hole, and the difference in energy between the higher-energy shell and the lower energy shell may be released in the form of an X-ray. The number and energy of the X-rays emitted from a specimen can be measured by an energy dispersive spectrometer. As the energy of the X-rays is characteristic of the difference in energy between the two shells, and of the atomic structure of the element from which they were emitted, this allows the elemental composition of the specimen to be measured. There are four primary components of the EDS setup: the beam source; the X-ray detector; the pulse processor; and the analyzer. Elements of low atomic number are difficult to detect by EDX. The EDX spectrum is just a plot of how frequently an X-ray is received for each

energy level. An EDX spectrum normally displays peaks corresponding to the energy levels for which the most X-rays had been received.

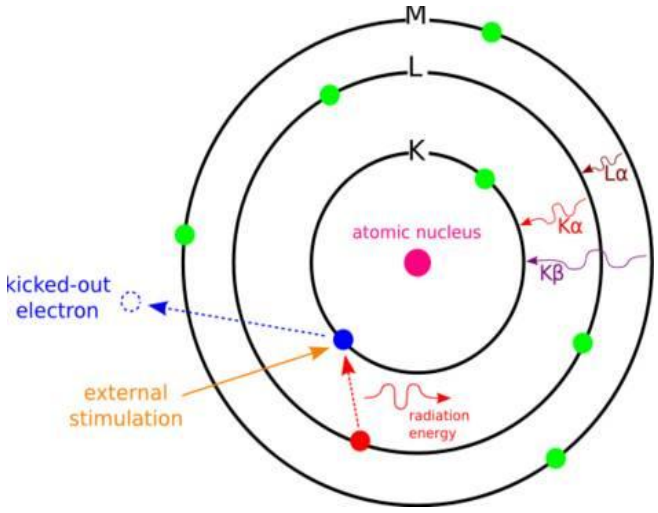

Figure 4.3 Different processes takes place when an electron interact with atom

Each of these peaks is unique to an atom, and therefore corresponds to a single element. The higher a peak in a spectrum, the more concentrated the element is in the specimen. An EDX spectrum plot not only identifies the element corresponding to each of its peaks, but the type of X-ray to which it corresponds as well.

4.2.3 Transmission Electron Microscope

Transmission Electron Microscopy is related technique that uses an electron beam to image a sample. High energy electrons, incident on ultra-thin samples allow for image resolutions that are on the order of 1 - 2 Angstroms. The image is magnified and focused onto an imaging device, such as a fluorescent screen, on a layer of photographic film. The transmission electron microscope uses a high energy electron beam transmitted through a very thin sample to image and analyze the microstructure of materials with atomic scale resolution. The electrons are focused with electromagnetic lenses and the image is observed on a fluorescent screen, or recorded on film or digital camera. The electrons are accelerated at several hundred kV, giving wavelengths much smaller than that of light: 200kV electrons have a wavelength of 0.025Å.

However, whereas the resolution of the optical microscope is limited by the wavelength of light, that of the electron microscope is limited by aberrations inherent in electromagnetic lenses, to about 1-2 Å. Because even for very thin samples one is looking through many atoms, one does not usually see individual atoms. Rather the high resolution

imaging mode of the microscope images the crystal lattice of a material as an interference pattern between the transmitted and diffracted beams.

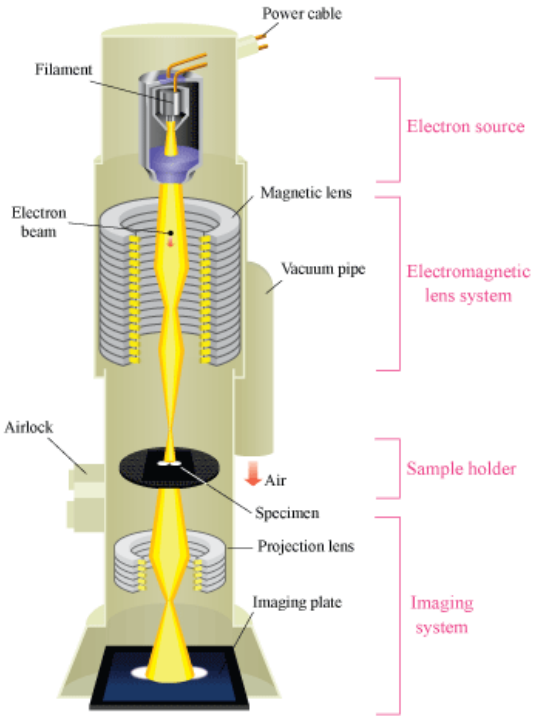

Figure 4.4 Schematic of different components of TEM

This allows one to observe planar and line defects, grain boundaries, interfaces, etc. with atomic scale resolution. The brightfield/darkfield imaging modes of the microscope, which operate at intermediate magnification, combined with electron diffraction, are also invaluable for giving information about the morphology, crystal phases, and defects in a material. Finally the microscope is equipped with a special imaging lens allowing for the observation of micromagnetic domain structures in a field-free environment.

It is used to find the morphology of the materials i.e the size, shape and arrangement of the particles which make up the specimen as well as their relationship to each other on the scale of atomic diameters.

4.2.4 UV-Visible absorption spectroscopy

UV-visible absorption spectroscopy involves the spectroscopy of photons in the UV-visible region. This means it uses light in the visible, near ultraviolet (UV) and near infrared ranges. When an incident beam reaches a medium, part of the beam will be reflected by the medium, part of the beam will be transmitted by the medium, and the rest of the beam will be absorbed. The absorption in the visible ranges directly affects the color of the chemicals

involved. In this region of the electromagnetic spectrum, molecules undergo electronic transitions. The wavelength of light that a compound will absorb is characteristic of its chemical structure. Specific regions of the electromagnetic spectrum are absorbed by exciting specific types of molecular and atomic motion to higher energy levels. Absorption of visible and ultraviolet (UV) radiation is associated with excitation of electrons, in both atoms and molecules, to higher energy states.

The Beer-Lambert law states that the absorbance of a solution is directly proportional to the concentration of the absorbing species in the solution and the path length. Thus, for a fixed path length, UV/VIS spectroscopy can be used to determine the concentration of the absorber in a solution. The amount of light, I, transmitted through a solution of an absorbing chemical in a transparent solvent can be related to its concentration by Beers Law:

$$- \log I/I_o = A = \varepsilon_\lambda \, bc$$

where I_o is the incident light intensity, A is the absorbance, b is the cell path length in cm, c is the solution concentration in moles/liter, and ε_λ is the molar absorptivity which has units of liter/mole/cm Notice that ε_λ is a function of wavelength, and it is the quantity which represents the spectrum of the solution. The type of transition takes place, when atoms interact with light.

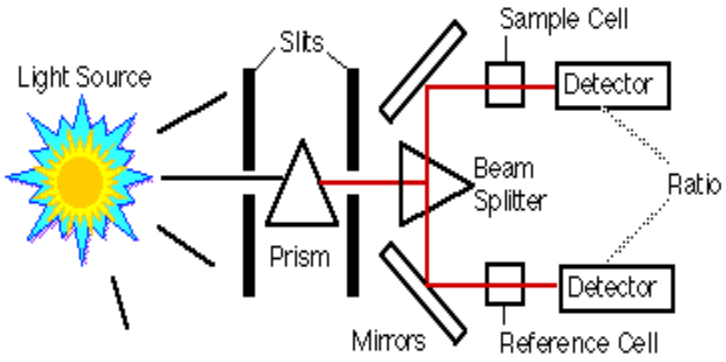

Figure 4.5 Schematic of UV-Visible spectrometer

It is used to find the absorbance, transmittance or reflectance of a material which can be further used to find extinction and dielectric coefficients, dielectric response function and refractive index of a material. It also used to find the band gap of a material.

4.2.5 Photoluminescence (PL)

Luminescence is the process where an electromagnetic radiation is produced by a substance under suitable external excitation. At certain frequencies, this radiation is significantly in excess of the thermal radiation, which is emitted by a substance at that particular temperature.

The so-produced electromagnetic radiation, generally in the visible region, is characteristic of the particular luminescent material under examination, termed as phosphor. The emission of visible light (400-700nm) corresponding to the region between red and violet requires excitation energies the minimum of which is given by Einstein's law stating that the energy, $E = h\nu = hc/\lambda$.

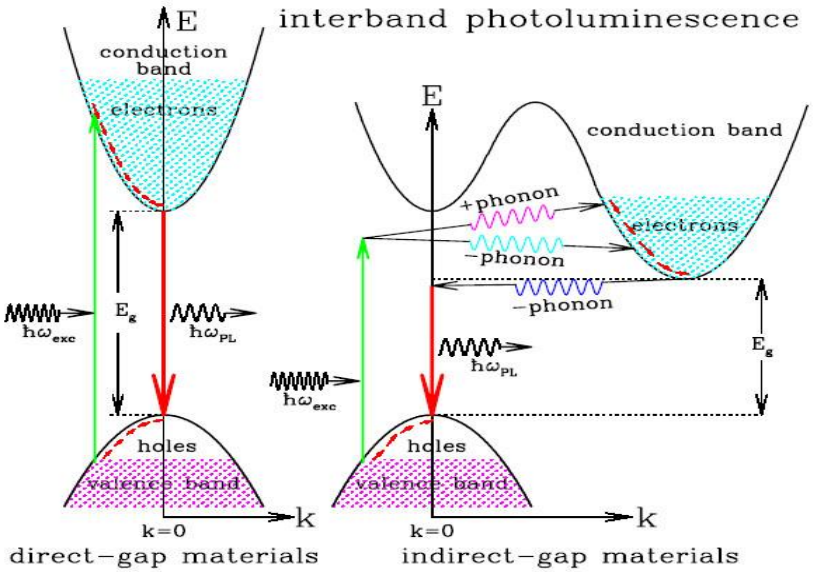

Figure 4.6 Interaction of light with semiconductor.

Luminescence is further subdivided into fluorescence and phosphorescence. A molecule in an excited state radiates energy after remaining in a metastable state for a fairly long time; the process is termed as phosphorescence. The luminescence process in which the molecule emits radiation as it falls directly from an excited state to a lower energy state is known as fluorescence. The time scale of the process is of the order of 10^{-8}s. Fluorescence radiation is due to allowed transitions ($\Delta S = 0$) from singlet excited state to the singlet ground state. If a molecule in an excited state radiates energy after remaining in a metastable state for a fairly long time, the process is termed as phosphorescence. The time scale of the phosphorescence process depends on the energy spacing between the metastable state and the nearest energy state to which transition is allowed and may be of the order of 10^{-6} seconds to minutes, hours or even days. This type of transition is due to forbidden transition ($\Delta S \neq 0$) from the excited metastable state to the lower ground state. It is used to find impurity levels, defect detection, recombination mechanisms and optical transition involves.

4.2.6 Fourier Transform Infrared Spectroscopy

Fourier Transform Infra-Red is the preferred method of infrared spectroscopy. In infrared spectroscopy, IR radiation is passed through a sample. Some of the infrared radiation is

absorbed by the sample and some of it is passed through (transmitted). The resulting spectrum represents the molecular absorption and transmission, creating a molecular fingerprint of the sample. Like a fingerprint no two unique molecular structures produce the same infrared spectrum. This makes infrared spectroscopy useful for several types of analysis. It is an analytical technique for the identification of organic and inorganic materials. It can be applied to the analysis of solids, liquids and gasses. Infrared spectroscopy detects the vibration characteristics of chemical functional groups in a sample. When an infrared light interacts with the matter, chemical bonds will stretch, contract and bend. As a result, a chemical functional group tends to absorb infrared radiation in a specific wavenumber range regardless of the structure of the rest of the molecule.

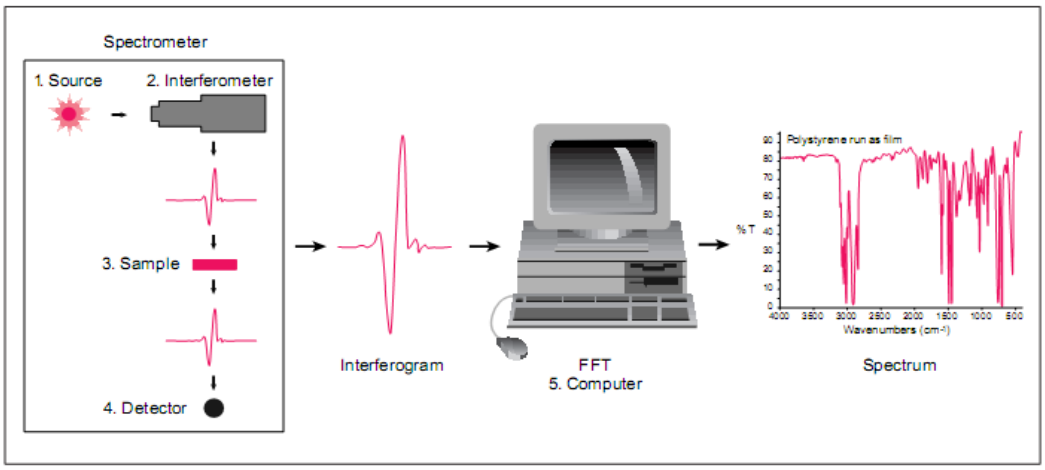

Figure 4.7 Schematic of FTIR

An infrared spectrum represents a fingerprint of a sample with absorption peaks which correspond to the frequencies of vibrations between the bonds of the atoms making up the material. Because each different material is a unique combination of atoms, no two compounds produce the exact same infrared spectrum. Therefore, infrared spectroscopy can result in a positive identification of every different kind of material. In addition, the size of the peaks in the spectrum is a direct indication of the amount of material present. A very simple optical device called an interferometer is used for measuring all of the infrared frequencies simultaneously, rather than individually. The interferometer produces a unique type of signal which has all of the infrared frequencies "encoded" into it. The signal can be measured very quickly. Most interferometers employ a beam splitter which takes the incoming infrared beam and divides it into two optical beams. The signal which exits the interferometer is the result of these two beams "interfering" with each other. The resulting signal is called an interferogram. As the interferogram is measured, all frequencies are being measured simultaneously. As the analyst requires a frequency spectrum in order to make

identification, the measured interferogram signal cannot be interpreted directly. A means of "decoding" the individual frequencies is required. This can be accomplished via a well-known mathematical technique called the Fourier transformation. This transformation is performed by the computer which then presents the user with the desired spectral information for analysis.

Uses of FTIR

- It can identify unknown materials.
- It can determine the quality or consistency of a sample.
- It can determine the amount of components in a mixture.

4.2.7 Vibrational Sample Magnetometer (VSM)

A vibrating sample magnetometer (VSM) is a scientific instrument that measures magnetic properties of materials as a function of magnetic field and temperature. A sample is placed inside a uniform magnetic field to magnetize the sample. The sample is then physically vibrated sinusoidal, typically through the use of a piezoelectric material. The induced voltage in the pickup coil is proportional to the sample's magnetic moment, but does not depend on the strength of the applied magnetic field. In a typical setup, the induced voltage is measured through the use of a lock-in amplifier using the piezoelectric signal as its reference signal. By measuring in the field of an external electromagnet, it is possible to obtain the hysteresis curve of a material.

A vibrating sample magnetometer (VSM) operates on Faraday's Law of Induction. If a sample of any material is placed in a uniform magnetic field, created between the poles of an electromagnet, a dipole moment will be induced. If the sample vibrates with sinusoidal motion a sinusoidal electrical signal can be induced in suitable placed pick-up coils. The signal has the same frequency of vibration and its amplitude will be proportional to the magnetic moment, amplitude, and relative position with respect to the pick-up coils system. The sample is fixed to a small sample holder located at the end of a sample rod mounted in a electromechanical transducer. The transducer is driven by a power amplifier which itself is driven by an oscillator at a frequency of 90 Hertz. The VSM employs an electromagnet which provides the magnetizing field (DC), a vibrator mechanism to vibrate the sample in the magnetic field and detection coils which generate the signal voltage due to the changing flux emanating from the vibrating sample. The output measurement displays the magnetic moment M as a function of the field H. The magnetic field is usually generated by an

electromagnet driven by a DC bipolar power supply. If extremely high magnetic fields are required (> 3T), the electromagnet is replaced by a superconducting solenoid. The voltage V measured across the sensing coils in a VSM can be expressed as the product off our contributing sources:

$$V = M \times A \times F \times S$$

Where, M = magnetic moment of the sample, A = amplitude of vibration, F = frequency of vibration and S = sensitivity function of the sensing coils.

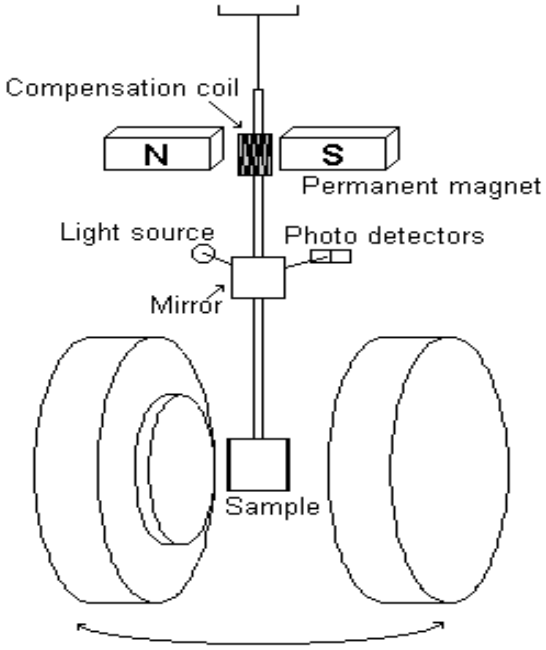

Figure 4.8 Schematic of components of VSM

Using a vibrating sample magnetometer one can measure the DC magnetic moment as a function of temperature, magnetic field, angle and time. So, it allows to perform susceptibility and magnetization studies. Some of the most common measurements done are: hysteresis loops, susceptibility or saturation magnetization as a function of temperature (thermomagnetic analysis), magnetization curves as a function as a function of angle (anisotropy), and magnetization as a function of time.

5.1 Structural and phase analysis

Figure 5.1 shows the XRD patterns of as synthesized CdSe and Cr doped CdSe nanoparticles. All the peaks are indexed and well matched to wurtzite structure having hexagonal phase with lattice parameters a = 4.299 A^o and c = 7.010 A^o which are in good agreement with the (JCPDS card no. 77-2307). The sharp diffraction peaks confirms the high crystallinity nature of nanoparticles.

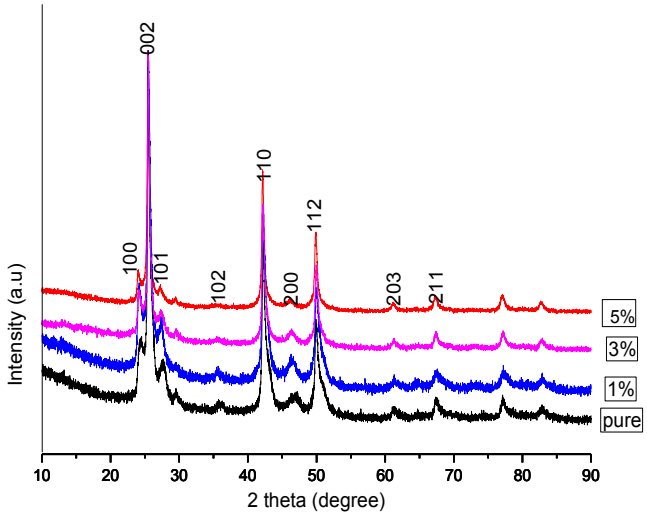

Figure5.1 XRD pattern of CdSe and Cr doped CdSe nanoparticles.

The crystallite size (D) of as synthesized nanoparticles is calculated by using Debye Scherrer formula given by

$$D = 0.94\,\lambda / \beta \cos\theta$$

where λ represents the wavelength of x-rays used, β is the full width at half maxima (FWHM). The calculated crystallite sizes are shown in the table 5.1

S. No	Doping %	Crystallite size (nm)
1	0	17.65
2	1	18.70
3	3	26.39
4	5	29.83

Table 5.1 Crystallite size variation with Cr doping.

The variation of crystallite size with Cr doping is shown in the figure 5.2. It is clear from the figure 5.2 that the crystallite size increases with increase in the Cr doping.

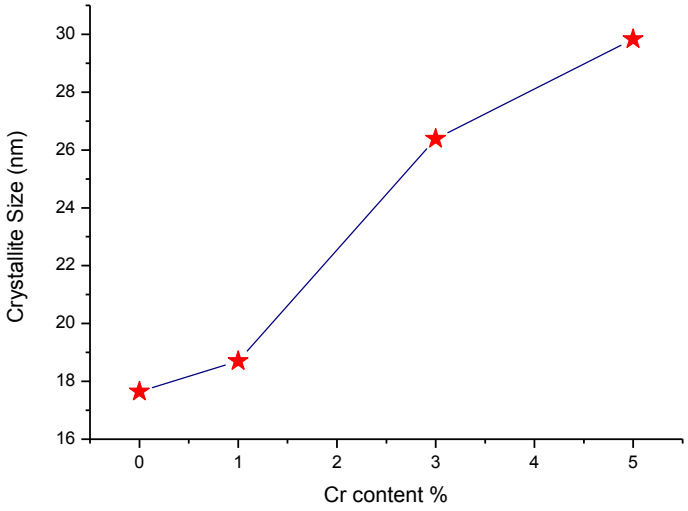

Figure 5.2 Variation of crystallites size with doping.

5.2 Morphological Study

5.2.1 SEM and EDAX analysis

The surface morphology of pure CdSe (figure 5.3 (a)) and Cr doped CdSe nanoparticles (figure (b) - (d)) are shown in figure 5.3. Figure 5.3 (a) reveals that CdSe nanoparticles are nearly spherical in shape but are in aggregated form but however with Cr doping in CdSe clearly indicates the formation of nanoclusters. The grains have aggregated to form clusters with larger size. The aggregation increases with increase in the doping. The average grain size diameters for Cr doped CdSe are found to be in the range of 2 ± 0.6μm.

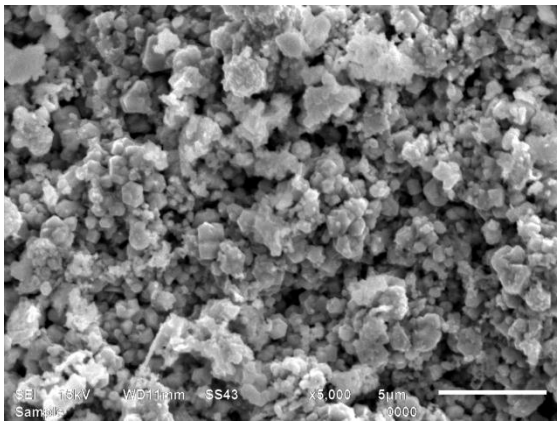

(a)

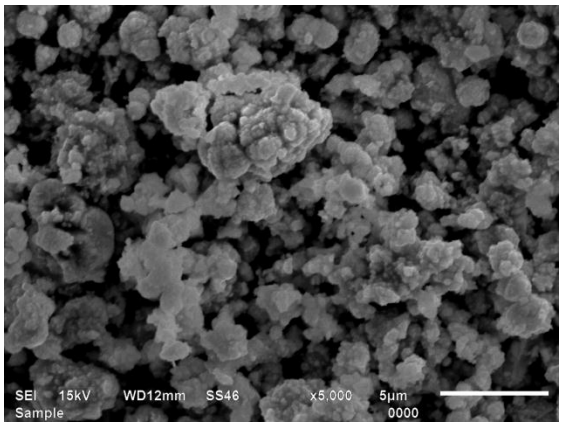

(b)

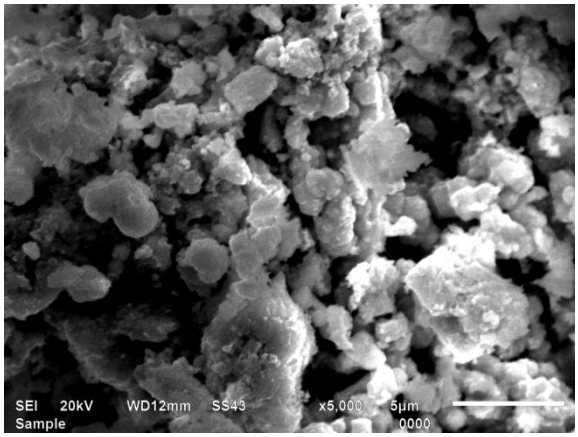

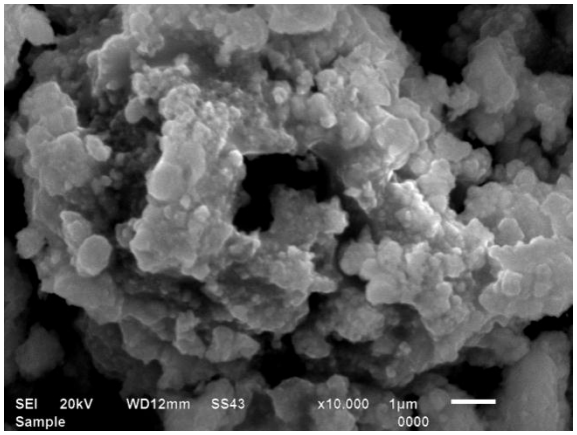

(c) (d)

Figure 5.3 SEM Micrograph (a) pure CdSe and Cr doped CdSe (b) 1% (c) 3% (d) 5% nanoparticles.

The chemical composition of the nanoparticles was analyzed by energy dispersive X-ray (EDAX) analysis. EDAX spectra of pure CdSe and Cr-doped CdSe nanoparticles are shown in figure 5.4. It is clear from figure 5.4 that Cd and Se are in stoichiometric ratio and therefore indicates the formation of pure CdSe. However but around 1.15 % and 3.22 % atomic percentage of Cr is detected in 1% and 3% Cr doped CdSe nanoparticles respectively.

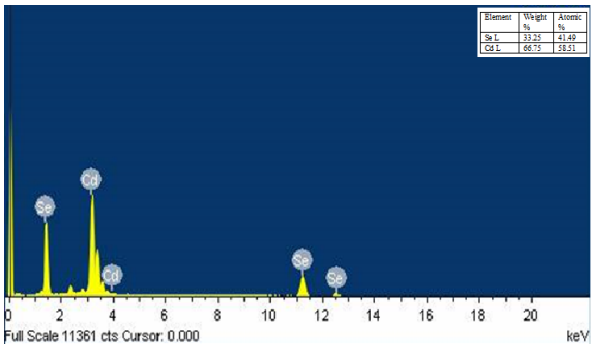

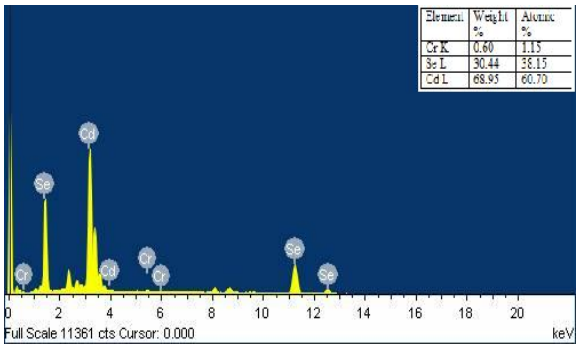

(a) (b)

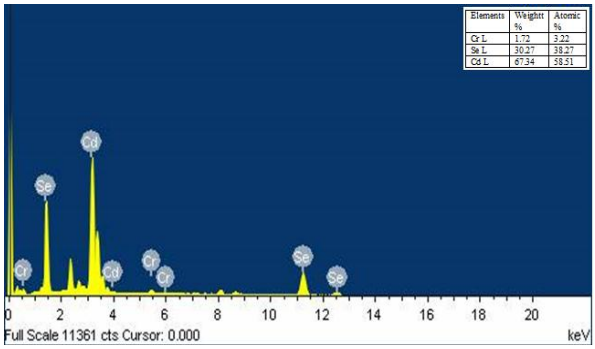

(c)

Figure 5.4 EDAX spectra of (a) pure CdSe (b) 1% and (c) 3% Cr doped CdSe nanoparticles.

5.2.2 TEM analysis

The morphological study of pure CdSe nanoparticles has been carried out by TEM. It's clear from the TEM micrograph (figure 5.5) that pure CdSe nanoparticles are nearly spherical in nature with average particle size 3.64 ± 0.86nm, moreover its clear from the figure (b) that size distribution follow gauss ion fit.

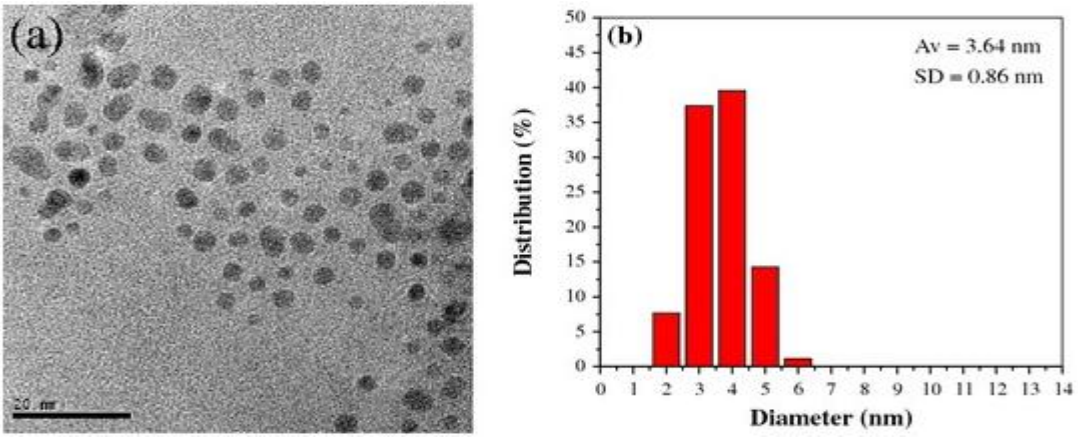

Figure5.5 (a) TEM micrograph of pure CdSe nanoparticles (b) size distribution of particles.

5.3 UV-Visible absorption study

The UV-visible absorption spectra of pure and Cr doped CdSe nanoparticles are shown in figure 5.6. It is clear from the spectra that absorption increases with addition of Cr in host CdSe nanoparticles and also absorption edge shows red shift.

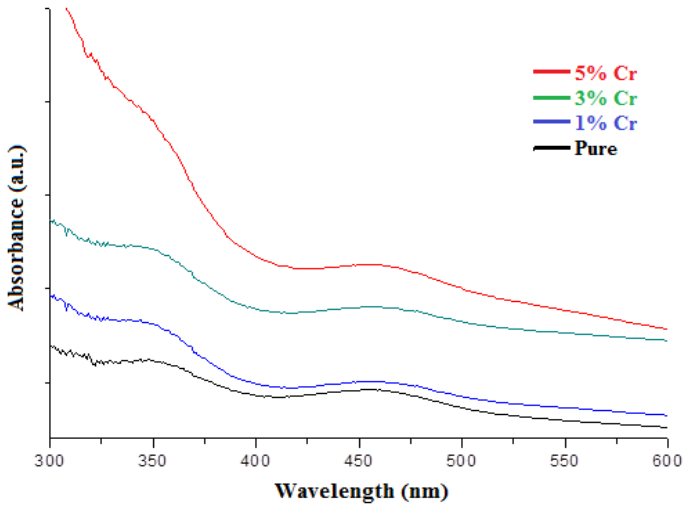

Figure 5.6 UV-Visible absorption spectra for pure CdSe and Cr doped CdSe nanoparticles.

The energy band gap of pure and Cr doped CdSe nanoparticles has been calculated from absorption edge tabulated in table 5.2. The band gap of bulk CdSe particle is 1.74eV but however the band gap value of pure CdSe nanoparticle has been found to be 3.12eV. The quantum confinement effects are responsible for the blue shift because of the localization of electrons and holes in the semiconductor nanocrystallites. This effect causes a change in the electronic band structure and consequently higher value of optical band gap is observed as compared to that of the bulk. Also its clear from the table 5.2 with addition of Cr a small change in band gap has been observed.

S.No	Doping %	Energy bandgap (eV)
1	0	3.12
2	1	3.14
3	3	3.16
4	5	3.20

Table 5.2 Variation of energy band gap with doping.

5.4 Photoluminescence study

The photoluminescence spectra of CdSe and Cr doped CdSe nanoparticles are shown in figure 5.7. The CdSe nanoparticles exhibit emission peak at 410 and 430 nm due to the near band-edge emission and a visible emission around 720 nm associated with the defects in CdSe.

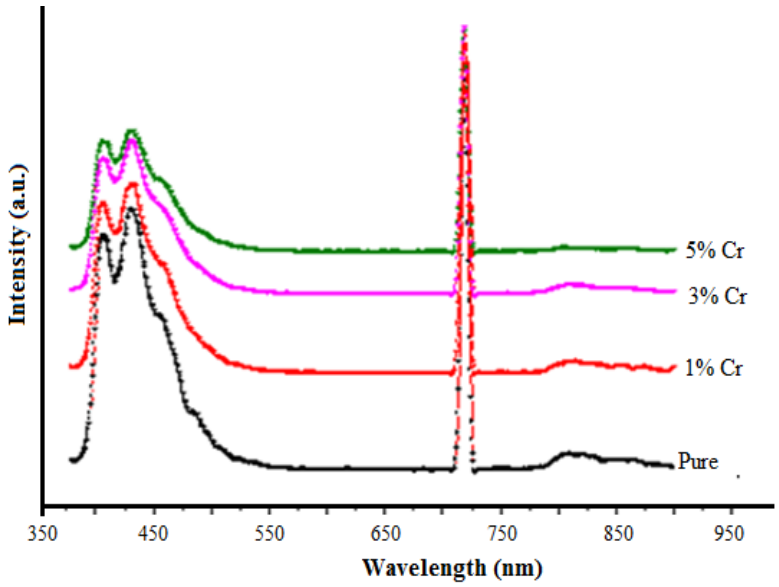

Figure 5.7 PL spectra of CdSe and Cr doped CdSe nanoparticles.

As the dopant concentration increases, the relative intensity of the visible emission increases significantly at higher Cr concentration. In addition to the band- edge and deep-level emission, a narrow emission peak at 720 nm with increased intensity at higher Cr concentration was observed. This peak may be attributed to the emission of Cr^{2+} ion internal transitions in CdSe.

5.5 FTIR study

Figure 5.8 shows the FTIR spectra of pure CdSe and Cr doped CdSe nanoparticles. The FTIR spectra show strong signal due to –OH, –SH, C–C, and $–CH_2$ present in case of the doped and undoped CdSe nanoparticles. The peak positions of the bonds are shown in figure 5.8. The spectra thus indicate that the doped as well as undoped nanoparticles are capped by marcaptoethanol molecules.

The peaks assigned due to different group present in FTIR spectra is shown in table 5.3. The peak positioned at 2555.14 cm^{-1} is due to –SH stretching vibration indicates 2-marcaptoethanol capped CdSe and Cr doped CdSe nanoparticles. This shows that the capping of 2- marcaptoethanol on CdSe and Cr doped CdSe nanoparticles is done. As the concentration of Cr increases more number of surface active sites is expected to be occupied by the Cr ions which bind strongly to the capping molecules.

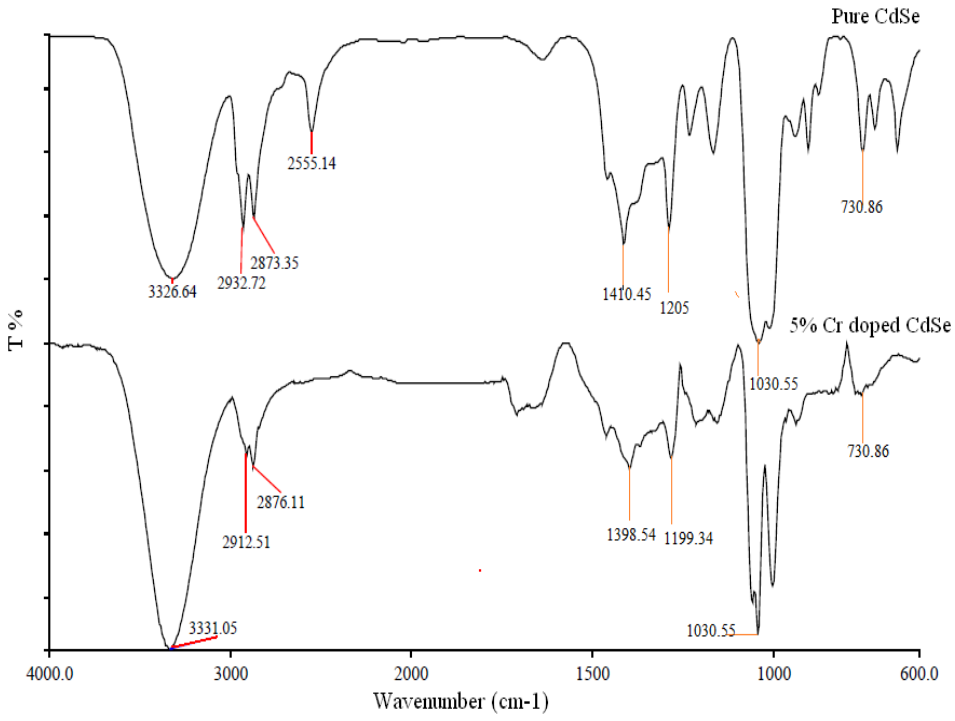

Figure 5.8 FTIR spectra of pure CdSe and Cr doped CdSe nanoparticles capped with 2-marcaptoethanol.

Peak position	Assignment
~ 3319	-OH stretching vibration
~ 2970-2750	-CH_2 and –CH_2 carbon/hydrogen stretching vibration
~ 2500	-SH stretching vibration
~ 1350-1450	-CH_2 and –CH_2
~ 1200-1250	Methylene wagging adjacent to thiol group
~ 1050-1000	-C-O-H stretching vibration
~ 790-620	-S-C- absorption

Table 5.3 FTIR mode assignments for 2-marcaptoethanol capping molecules.

5.6 Magnetic study

The magnetic study has been carried out at room temperature using VSM as shown in a figure 5.9.It is clear from the figure 5.9 (a) that pure CdSe nanoparticles exhibit diamagnetic behaviour at room temperature but however with 5% doping of Cr in the host CdSe shows ferromagnetic character with saturation magnetization value is0.168 emu/g, remnant magnetization is 0.05 emu/g and coercive field is 186.72 Oe.

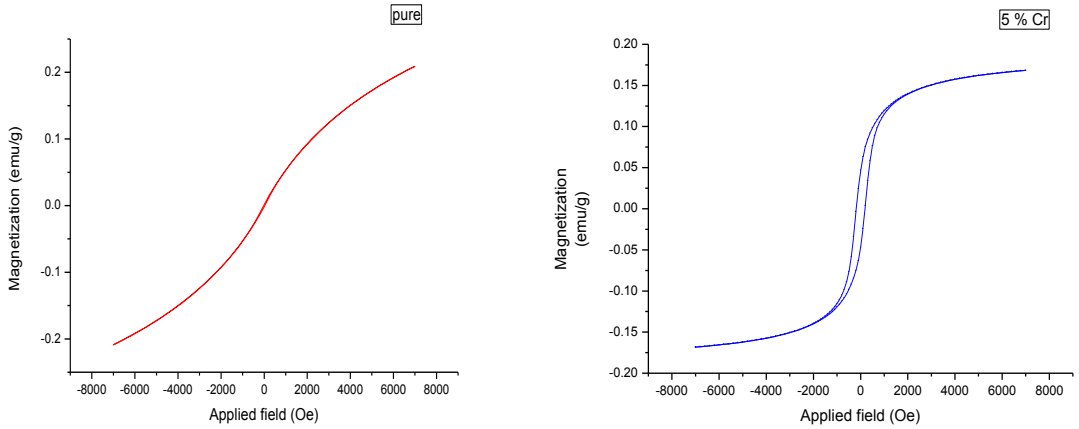

(a) (b)

Figure5.9 Magnetic hysteresis (M–H) loops for (a)pure CdSe and (b) 5% Cr doped CdSe nanoparticles measured at 300 K.

5.7 Conclusions

In the present work, pure and Chromium (Cr) doped CdSe nanoparticles have been synthesized by solvothermal method using 2-marcaptoethanol as a capping agent.

- ✓ XRD analysis shows that the prepared samples are in hexagonal wurtzite phase. The particle size can be adjusted by controlling the dopant concentration. The average size of nanoparticle increases as the doping percentage of Cr is increased.
- ✓ UV-visible absorption study reveals that the energy band gap value increases with increase in Cr dopant concentration. Optical absorption measurements indicate red shift in the absorption band edge upon Cr doping.
- ✓ The particle size distributions were studied by TEM.TEM study reveals that the nanoparticles are spherical in shape with average particle size is 3.64 ± 0.86 nm.
- ✓ Incorporation of Cr in the CdSe nanoparticles was confirmed by EDX study.
- ✓ Magnetic study reveals that, M-H curve of pure CdSe nanoparticles are showing diamagnetic as no saturation in M-H curve is observed but, however with addition of 5% of Cr in CdSe they show ferromagnetic behavior. The exchange interactions between Cr ions mediated by carriers contribute to the ferromagnetism at room temperature.

References

[1] N. Lane, J. Nano. Res. 3 (2001) 95.

[2] T. Dietl, J. Phys. Condens. Matter. 19 (2007) 165204.

[3] C. Liu, F. Yun, H. Morkoc, J. Mat. Sci. 16 (2005) 555.

[4] S.D. Bader, S.S.P. Parkin, Annu. Rev. Condens. Matter Phys. 1 (2010) 71.

[5] S. Datta, B. Das, Appl. Phys. Lett. 56 (1990) 665.

[6] G. Binash, P. Grunberg, F. Saurenbach, W. Zinn, Phys. Rev. B 39 (1989) 2527.

[7] A. Fert, Thin Solid Films 517 (2008) 2.

[8] K. F. Wang, J. M. Liu, Z. F. Ren, Nature 442 (2009) 759.

[9] R. W. Meulenberg, J R. I. Lee, S. K. McCall, K. M. Hanif, D. Haskel, J. C. Lang, L. J. Terminello, T. V. Buure, J. Am. Chem. Soc. 131 (2009) 6888.

[10] V. A. Ivanov, Bulletin of the Russian Academy of Sciences: Physics 71 (2007) 1610.

[11] T. Dietl, H. Ohno, Mater. Res. Soc. Bull. 28, (2003) 714.

[12] S.J. Pearton1, C.R. Abernathy, D.P. Norton, A. F. Hebard, Y.D. Park, L.A. Boatner, J.D. Budai, J. Mater. Sci. Eng. R 40 (2003) 137.

[13] J. M. D. Coey, J. Curr. Opin. Solid State Mater. Sci.10 (2006) 83.

[14] V. A. Ivanov, E. A. Ugolkova, O. N. Pashkova, V. P. Sanygin, A. G. Padalko, J. Magn. Magn. Mater 300 (2006) e32.

[15] R. Beaulac, P. I. Archer, S. T. Ochsenbein, D. R. Gamlin, Adv. Funct. Mater. 18 (2008) 3873.

[16] F. V. Mikulec, M. Kuno, M. Bennati, D. A. Hall, R. G. Griffin, M. G. Bawendi, J. Am. Chem. Soc. 122 (2000) 2532.

[17] K. M. Hanif, R. W. Meulenberg, G. F. Strouse, J. Am. Chem. Soc. 124 (2002) 11495.

[18] W. B. Jian, J. Fang, T. Ji, Appl. Phys. Lett. 83 (2003) 3377.

[19] R. W. Meulenberg, T. V. Buuren, K. M. Hanif, T. M. Willey, G. F. Strouse, L. J. Terminello, Nano Lett. 4 (2004) 2277.

[20] D. Magana, S. C. Perera, A. G. Harter, N. S. Dalal, G. F. Strouse, J. Am. Chem. Soc. 128 (2006) 2931.

[21] P. I. Archer, S. A. Santangelo, D. R. Gamelin, Nano Lett. 7 (2007) 1037.

[22] S. B. Singh, M. V. Limaye, S. K. Date, S. K. Kulkarni, J. Chem. Phys. Lett. 464 (2008) 208.

[23] M. S. Seehra, P. Dutta, S Neeleshwar, Y. Y Chen, C. L. Chen, S. W. Chou, C. C. Chen, C. L. Dong, C. L. Chang, J. Adv. Mater. 20 (2008) 1656.

[24] Y. Niwayama, H. Kura, T. Sato, M. Takahashi, T. Ogawa, Appl. Phys. Lett. 92

(2008**)** 202502.

[25] S. B. Singh, M. V. Limaye, S. K. Date, S. Gokhle, S. K. Kulkarni, J. Phys. Rev. B 80 (2009) 235421.

[26] S Kumar, S. Kumar, N. K. Verma, S. K. Chakarvarti, J. Mater Sci: Mater. Electron. DOI 10.1007/s10854-010-0233-5.

[27] R. W. Meulenberg, J. R. I. Lee, S. K. McCall, D. Haskel, J. C. Lang, L. J. Terminello, T. V. Buuren, J. Electrochem. Soc. 28 (2010) 203.

[28] L. Jun, C. Li, L. Yu, D. H. Ning, Z. R. Lun, J. Chin. Phys. B 19 (2010) 037103.